Pure Appl. Chem., Vol. 85, No. 2, pp. 385–396, 2013.
http://dx.doi.org/10.1351/PAC-CON-12-07-10

Lower- and upper-rim-modified derivatives of 1,3,5-triaza-7-phosphaadamantane: Coordination chemistry and applications in catalytic reactions in water*

Luca Gonsalvi[1,‡], Antonella Guerriero[1], Frédéric Hapiot[2], Donald A. Krogstad[3], Eric Monflier[2], Gianna Reginato[1], and Maurizio Peruzzini[1,‡]

[1]Consiglio Nazionale delle Ricerche, Istituto di Chimica dei Composti Organometallici (ICCOM-CNR), Via Madonna del Piano 10, 50019 Sesto Fiorentino (Firenze), Italy; [2]Université Lille Nord de France, CNRS UMR 8181, Unité de Catalyse et de Chimie du Solide, UCCS UArtois, Faculté Jean Perrin, rue Jean Souvraz, SP18, F-62300 Lens, France; [3]Concordia College at Moorhead, 334F Ivers, Moorhead, MN 56562, USA

Abstract: In this article, a brief review of the recent functionalizations of the cage-like water-soluble phosphine 1,3,5-triaza-7-phosphaadamantane (PTA), involving *N*-quaternization (lower rim) and introduction of a side arm in C-6 position (upper rim) will be presented, highlighting selected examples in their use as ligands for ruthenium(II), iridium(I), and rhodium(I) moieties together with applications of the related complexes in homogeneous catalysis.

Keywords: homogeneous catalysis; hydroformylation; hydrogenation; organometallic chemistry; transition metals; water.

INTRODUCTION

During the past few years, the neutral water-soluble cage monodentate phosphine PTA (PTA = 1,3,5-triaza-7-phosphaadamantane) [1] and its structural modifications have found large attention by many research groups, as recently reviewed [2]. A variety of coordination compounds have been synthesized, and their catalytic [3], medicinal [4], and electrochemical properties [5] have been assessed, together with mechanistic aspects of ruthenium-PTA mediated hydrogen activation in water [6].

It has also been shown that this aminophosphine can be considered as a versatile scaffold for many different structural modifications, which in turn can change the electronic, steric, binding properties and water solubility of the parent compound.

Our collaborative work in recent years has led to the development of novel PTA-like derivatives and their application as ligands for transition metals endowed with catalytic properties such as ruthenium(II), iridium(I), and rhodium(I), namely, C=C and C=O bonds hydrogenation and transfer hydrogenations under mild conditions, and biphasic hydroformylation of higher olefins in the presence of cyclodextrins (CDs) as mass transfer promoters.

Pure Appl. Chem.* **85, 315–462 (2013). A collection of invited papers based on presentations at the 12th Eurasia Conference on Chemical Sciences, Corfu, Greece, 16–21 April 2012.
‡Corresponding authors: E-mail: l.gonsalvi@iccom.cnr.it; maurizio.peruzzini@iccom.cnr.it

Hereby are summarized our recent contributions highlighting the synthetic protocols developed by us and other authors to obtain PTA functionalization at carbon in 6-position, i.e., close to the phosphorus donor atom, and tailored *N*-quaternizations of PTA (Scheme 1), which have been exploited to interact selectively with CDs in a temperature-dependent manner.

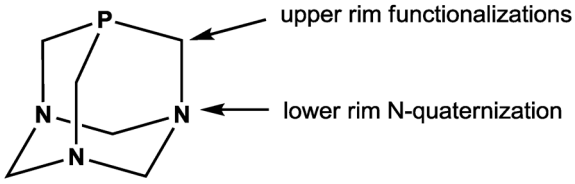

Scheme 1 PTA upper- and lower-rim modifications.

UPPER-RIM PTA FUNCTIONALIZATIONS

Ligand synthesis and coordination chemistry

The access to C6-functionalization of PTA was made possible by the discovery of its selective reactivity with *n*-butyllithium to yield 1,3,5-triaza-7-phosphaadamantane-6-yl lithium, PTA-Li (**1**), originally published by Frost and co-workers [7]. In this first article, the authors reacted it with $ClPPh_2$ in 1,2-dimethoxyethane giving the racemic bidentate phosphine PTA-PPh_2 (**2**) in low isolated yields. The bidentate properties of this ligands were demonstrated by reaction with *cis*-$[M(CO)_4(NHC_5H_{10})_2]$ (M = Mo, W) in degassed dichloromethane (Scheme 2). This gave, as expected, the chelate complexes $[M(CO)_4$(PTA-$PPh_2)]$ (**3**, M = Mo, W).

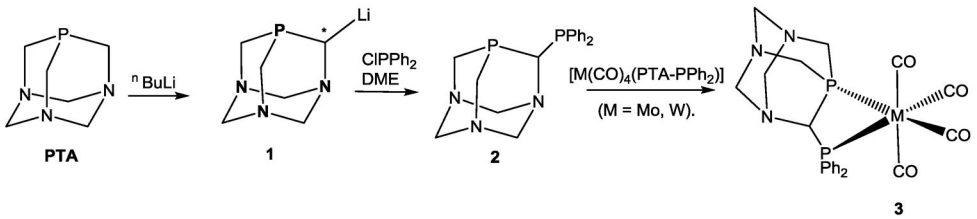

Scheme 2 Synthesis of PTA-Li (**1**), PTA-PPh_2 (**2**), and $[M(CO)_4$(PTA-$PPh_2)]$ (**3**, M = Mo, W).

Different electrophiles such as ketones, aldehydes, and CO_2 were inserted into the C–Li bond of **1**, giving a small library of racemic water-soluble β-phosphino alcohols either of general formula PTA-CR_2OH (R = Ph, C_6H_4OMe, Scheme 3) bearing one stereocenter at the cage C atom, or PTA-CH(R)OH (R = Ph, C_6H_4OMe, ferrocenyl) having two stereogenic carbon atoms, or carboxylates PTA-CO_2X (X = Li, Me), respectively. Several of these phosphines were subsequently reacted with $[Ru(\eta^6\text{-}C_6H_5R)Cl_2]_2$ (R = H, Me) to form complexes of the general form $[(\eta^6\text{-}C_6H_5R)RuCl_2$(phosphine)] (Scheme 3). The reaction of **1** with aryl aldehydes was independently reported at about the same time by Frost and some of us [8]. In particular, in our laboratories, the ligand PZA (PZA = phenyl-(1,3,5,-triaza-7-phosphatricyclo[3.3.1.1]dec-6-yl)methanol) was reacted with $[Cp^*IrCl_2]_2$ to give the corresponding iridium(III) complex $[Cp^*Ir(PZA)Cl_2]$ (**4**) where the phosphine showed, as expected, a κ^1-P coordination mode (Scheme 3).

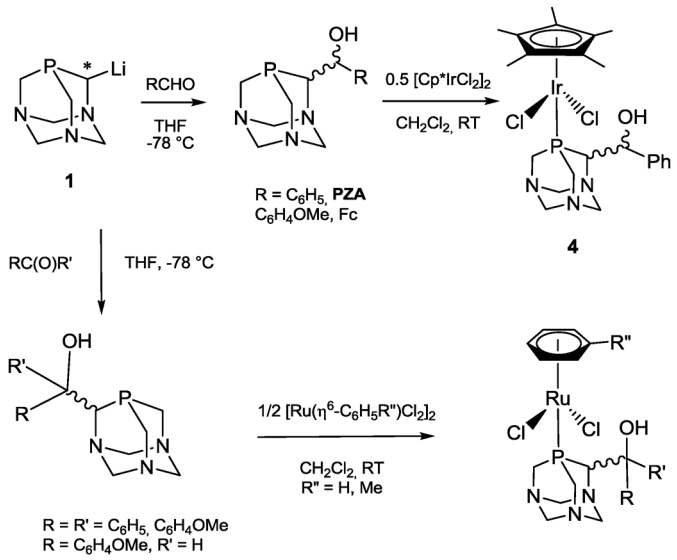

Scheme 3 Synthesis of racemic upper-rim PTA derivatives and related Ru(II) and Ir(III) complexes.

Encouraged by these initial results, we then decided to react **1** with other aryl aldehydes bearing different substituents, for example, on the phenyl ring, in order to test the changes in the electronic, steric, and coordination abilities toward transition-metal fragments of interest in catalysis. Thus, reaction of **1**, isolated as pure pyrophoric solid by running the lithiation of PTA in warm benzene under nitrogen, with 4-(dimethylamino)benzaldehyde gave the new water-soluble ligand 4'-(dimethylamino)phenyl-(1,3,5,-triaza-7-phosphatricyclo[3.3.1.1]dec-6-yl) methanol (PZA-NMe_2). By fractional crystallization, it was possible to separate the two diastereoisomers, in particular the (*SR*,*RS*)-isomer (**5**) was obtained in good yields and purity.

The coordination properties of PZA and **5** were tested by reaction with $[Ir(cod)Cl]_2$ and $[Ru(\eta^6\text{-}p\text{-cymene})Cl_2]_2$, respectively (Scheme 4). The corresponding κ^1-P complexes [Ir(cod)Cl(PZA)] (**6**), [Ir(cod)Cl{(*SR*,*RS*)-(PZA-NMe_2)}] (**7**), [(η^6-*p*-cymene)$RuCl_2$(PZA)] (**8**), and [(η^6-*p*-cymene)$RuCl_2${(*SR*,*RS*)-(PZA-NMe_2)}] (**9**) were obtained in moderate to good yields and fully characterized [9,10].

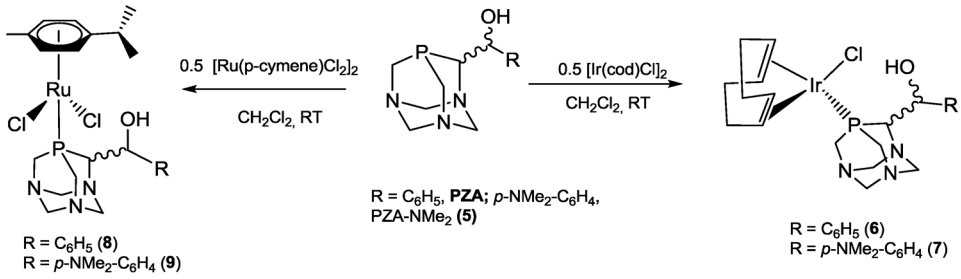

Scheme 4 Synthesis of κ^1-P complexes [Ir(cod)Cl(PZA)] (**6**), [Ir(cod)Cl{(*SR*,*RS*)-(PZA-NMe_2)}] (**7**), [(η^6-*p*-cymene)$RuCl_2$(PZA)] (**8**), and [(η^6-*p*-cymene)$RuCl_2${(*SR*,*RS*)-(PZA-NMe_2)}] (**9**).

The possibility to force κ^2-P,O chelation in **7** was tested by reaction with a chloride scavenger ($TlPF_6$) in dichloromethane at room temperature. $^{31}P\{^1H\}$ NMR data showing a shift from –64.1 ppm due to **7** to –17.04 ppm was attributed to the formation of the cationic complex κ^2-P,O-[Ir(cod){(*SR*,*RS*)-(PZA-NMe_2)}]$^+$. The possible κ^2-P,O coordination was confirmed by reaction of **5** with the iridium(I) precursor $[Ir(cod)_2]PF_6$ in a 1:1 ratio in dichloromethane at room temperature, which gave the same $^{31}P\{^1H\}$ NMR signal at –17.04 ppm. Due to the acidity of the OH proton and the basicity of the N atoms in the triazacyclohexane bottom rim on the PTA skeleton, a protonation–deprotonation intermolecular equilibrium was also proposed to be active (Scheme 5). Density functional theory (DFT) theoretical calculations were used to assess the energies associated with a protonation–deprotonation intermolecular equilibrium, confirming the experimental results [9].

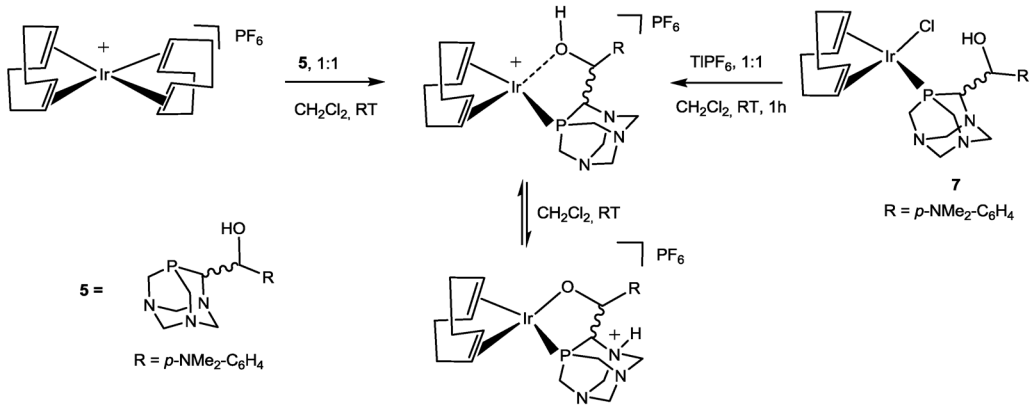

Scheme 5 Mechanism for the switch from κ^1-P to κ^2-P,O coordination mode in **7**.

Following in our research, **1** was reacted with 1-methyl-2-imidazolecarboxaldehyde and bis(*N*-methylimidazole-2-yl)ketone, respectively. The novel water-soluble mono-imidazolyl upper-rim functionalized PTA derivative, 1'-methylimidazolyl-(1,3,5-triaza-7-phosphatricyclo[3.3.1.1^{3,7}]dec-6-yl)methanol [**10**, PTA-CH(1-MeIm)OH], and the bis-imidazolyl analogue, bis-1'-methylimidazolyl-(1,3,5-triaza-7-phosphatricyclo [3.3.1.1^{3,7}]dec-6-yl)methanol [**11**, PTA-C(1-MeIm)$_2$OH], were obtained in moderate yields and good purity after workup. By reaction with [Ru(η^6-*p*-cymene)Cl_2], the corresponding κ^2-*P*,*N*-[(η^6-*p*-cymene)Ru{PTA-CH(1-MeIm)OH}Cl]Cl (**12**) and κ^2-*P*,*N*-[(η^6-*p*-cymene)Ru{PTA-C(1-MeIm)$_2$OH}Cl]Cl (**13**) were obtained in good yields (Scheme 6). In the case of imidazolyl-PTA derivatives, κ^2-*P*,*N* coordination is preferred. These experimental findings were explained by DFT calculations, suggesting that the higher chelating properties of **10** and **11** may be due to the softer nature of the N atom on the imidazole ring compared to both O hydroxyl and adamantane cage N atoms [10].

The iridium(I) and ruthenium(II) complexes described were tested as catalysts for C=C and C=O bonds hydrogenation and transfer hydrogenations under mild conditions, and the most relevant results are hereby summarized.

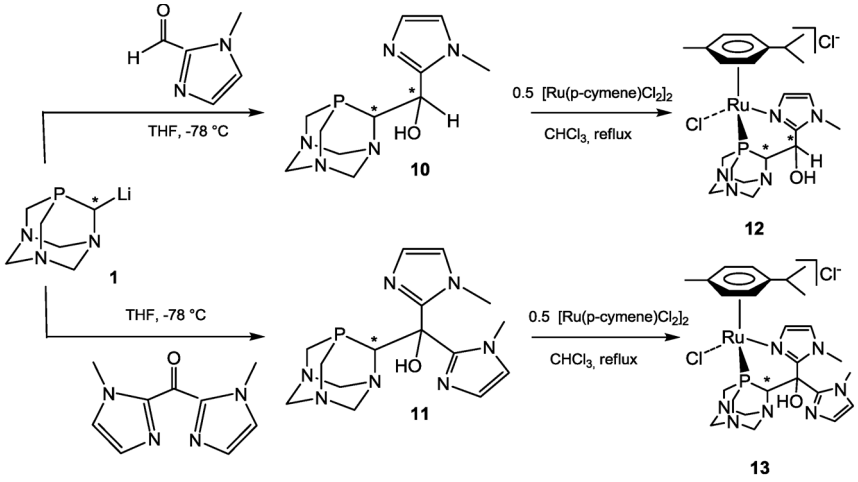

Scheme 6 Synthesis of PTA-CH(1-MeIm)OH (**10**), PTA-C(1-MeIm)$_2$OH (**11**), and related κ^2-*P*,*N* Ru(arene) complexes.

Catalytic hydrogenations with iridium(I) and ruthenium(II) upper-rim complexes

We have tested complex **7** as a catalyst for the chemoselective hydrogenation of model substrates including linear α,β-unsaturated (benzylidene acetone, BZA) and cyclic ketones (2-cyclohexen-1-one) and simple aryl alkyl ketones (acetophenone) using different reduction protocols. Transfer hydrogenation of BZA using sodium formate in water/methanol at 60 °C in the presence of **7** (1:100 catalyst to substrate ratio) showed a maximum conversion of ca. 55 % at 24 h and a ca. 4:1 ratio between saturated ketone and unsaturated alcohol was reached (Table 1, entries 1,2). For transfer hydrogenation of 2-cyclohexen-1-one, both the sodium formate/water/methanol protocol (Table 1, entry 2) and the potassium hydroxide/isopropanol method (Table 2, entries 4,5) were applied in the presence of **7**, using cat-

Table 1 Selected data for transfer hydrogenation of BZA, 2-cyclohexen-1-one, and acetophenone with **7**.

Entry	Substrate		Yields				
		% Conv (h)	% A[c]	% B[c]	% C[c]	TON (avg)	TOF (h^{-1})
1	BZA[a]	55.1 (24)	43.7	11.5	0.0	55	2.29
2	2-Cyclohexen-1-one[a]	67.4 (24)	57.9	0.2	6.3	67	2.79
3	2-Cyclohexen-1-one[a,d]	64.4 (24)	60.0	0.2	7.2	64	2.67
4	2-Cyclohexen-1-one[b]	83.3 (5)	24.9	0.6	57.8	208	41.6
5	2-Cyclohexen-1-one[b]	88.1 (24)	16.3	0.5	71.3	220	9.2
6	2-Cyclohexen-1-one[b,d]	79.6 (5)	29.5	0.5	49.6	199	39.8
7	2-Cyclohexen-1-one[b,d]	87.8 (24)	22.0	0.5	65.3	220	9.2
8	Acetophenone[b]	84.5 (5)	84.5	–	–	211	42.2
9	Acetophenone[b]	94.5 (24)	94.5	–	–	236	9.8
10	Acetophenone[b,d]	83.8 (5)	83.8	–	–	210	42.0
11	Acetophenone[b,d]	94.2 (24)	94.2	–	–	236	9.8

[a]Conditions: substrate, 0.75 mmol; catalyst, 7.5×10^{-3} mmol; HCO_2Na, 7.5 mmol; MeOH/H_2O (1:1), 6 mL.
[b]Conditions: substrate, 4.40 mmol; catalyst, 8.8×10^{-3} mmol; KOH, 0.88 mmol; ^{i}PrOH, 8.8 mL.
[c]GC values based on pure samples. For BZA, A = 4-phenyl-2-butanone; B = 4-phenyl-3-buten-2-ol; C = 4-phenyl-2-butanol, T = 60 °C. For 2-cyclohexen-1-one, A = cyclohexanone; B = 2-cyclohexen-1-ol; C = cyclohexanol, T = 80 °C. For acetophenone, A = 1-phenylethanol, T = 80 °C.
[d]One drop of Hg(0) added. Reprinted (adapted) with permission from ref. [9]. Copyright © 2011 American Chemical Society.

Table 2 Selected data for hydrogenations with **7** in ^{i}PrOH/^{t}BuOK under a pressure of H_2.

Entry	Substrate	% Conv (h)	Yields % A[b]	% B[b]	% C[b]	TON(avg)	TOF (h^{-1})
1	Acetophenone[a]	94.1 (6)	94.1	–	–	240	40.0
2	Acetophenone[a,c]	76.2 (4)	76.2			191	47.8
3	2-Cyclohexen-1-one[a]	60.1 (4)	42.5	0.9	16.7	150	37.5
4	2-Cyclohexen-1-one[a,c]	59.5 (4)	36.0	0.4	23.1	149	37.3

[a]Conditions: substrate, 1.75 mmol; catalyst, 7.0×10^{-3} mmol; ^{t}BuOK , 0.35 mmol; ^{i}PrOH, 2 mL. $p(H_2)$, 30 bar, 25 °C.
[b]GC values based on pure samples. For 2-cyclohexen-1-one, A = cyclohexanone; B = 2-cyclohexen-1-ol; C = cyclohexanol. For acetophenone, A = 1-phenylethanol.
[c]Hg(0) added. Reprinted (adapted) with permission from ref. [9]. Copyright © 2011 American Chemical Society.

alyst:substrate ratios of 1:100 and 1:500, respectively. In the first case, selective hydrogenation to cyclohexanone was observed, giving a maximum conversion of 67 % after 24 h. By running the test using potassium hydroxide as base, after 24 h at 80 °C, selective reduction to cyclohexanol was achieved (71 % yield) with a turnover number (TON) = 220. Acetophenone was also reduced to 1-phenylethanol using potassium hydroxide/isopropanol under the same conditions with a maximum TON = 236 (Table 1, entry 9). The true homogeneous nature of the catalyzed processes was proven by repeating selected runs in the presence of elemental mercury.

Another set of conditions for hydrogenation of unsaturated substrates, namely, potassium *tert*-butoxide/isopropanol under hydrogen pressure (30 bar) at room temperature, was tested for the reduction of acetophenone and 2-cyclohexen-1-one in the presence of **7** (Table 2). Almost complete conversion of acetophenone to 1-phenylethanol was reached after 6 h, whereas 2-cyclohexen-1-one was reduced with a maximum conversion of ca. 60 % after 4 h, mainly giving the C=C hydrogenation product.

Ruthenium(II) complexes **8**, **9**, **12**, **13** showed moderate to very good activities for the reduction of acetophenone under very mild conditions, as summarized in Table 3, using as little catalyst as 0.1 % in the case of **12** (Table 3, entry 8).

Table 3 Selected results for the hydrogenation of acetophenone catalyzed by **8**, **9**, **12**, **13** under a pressure of H_2 in ^{t}BuOK/^{i}PrOH or KOH/H_2O.

Entry	Catalyst	Solvent	Cat/sub/base	Base	Temperature (°C)	Time (h)	Conversion (%)[b]
1	**8**[a]	^{i}PrOH	1/250/50	^{t}BuOK	25	4	26.1
2	**8**[c]	^{i}PrOH	1/250/5	^{t}BuOK	80	4	95.3
3	**9**[a]	^{i}PrOH	1/250/50	^{t}BuOK	25	4	2.0
4	**9**[c]	H_2O	1/250/10	KOH	60	4	25.4
5	**9**[c]	^{i}PrOH	1/250/5	^{t}BuOK	80	4	92.9
6	**9**[c,d]	^{i}PrOH	1/250/5	^{t}BuOK	80	4	95.9
7	**12**[a,d]	^{i}PrOH	1/250/5	^{t}BuOK	25	4	82.0
8	**12**[c]	^{i}PrOH	1/1000/5	^{t}BuOK	40	4	89.7
9	**12**[c]	^{i}PrOH	1/250/5	^{t}BuOK	60	1	100
10	**12**[c]	^{i}PrOH	1/500/5	^{t}BuOK	60	4	100
11	**12**[c]	H_2O	1/250/5	KOH	60	4	38.2
12	**13**[c]	^{i}PrOH	1/250/5	^{t}BuOK	60	4	53.0
13	**13**[c]	^{i}PrOH	1/250/5	^{t}BuOK	80	4	96.9

[a]Solvent, 2 mL; pH_2, 30 bar; catalyst 7.0×10^{-3} mmol.
[b]Conversions determined by GC based on pure samples.
[c]Solvent, 40 mL; pH_2, 30 bar; catalyst 2.6×10^{-2} mmol.
[d]Addition of Hg(0). Reprinted (adapted) with permission from ref. [10]. Copyright © 2011 American Chemical Society.

LOWER-RIM FUNCTIONALIZATIONS

Many different lower-rim PTA functionalizations have been described in the literature and have been recently reviewed [2]. In the following section, a very specific example of *N*-quaternization will be described, highlighting the possible application in catalysis of the novel ligands obtained by this simple modification of the PTA structure.

Ligand synthesis and interaction studies with cyclodextrins (CDs)

The use of catalytic processes run in a biphasic water/organic phase environment has received interest both from academic and industrial points of view. A classic example is the Rhurchemie/Rhône-Poulenc process for which the hydroformylation of propene or butene was possible in water by the use of water-soluble organometallic catalysts [11]. However, the majority of organic substrates are not soluble in aqueous media. As a possible solution, the use of CDs proved to be of particular interest since these torus-like glucopyranosidic macro-rings can improve the mass transfer between the substrate-containing organic phase and the catalyst-containing aqueous one [12].

However, the efficiency of CD-based biphasic system may be hampered by detrimental interactions between the CD and the water-soluble ligand that stabilize the catalyst in water, as in the case of TPPTS ligand [TPPTS = tris(sulfonatophenyl)phosphine], which can be trapped in the cavity of the randomly methylated β-CD (RAME-β-CD) and in turn decrease the hydroformylation regioselectivity [13]. For this reason, non-interacting water-soluble phosphines should be preferred for this process.

At first, we tested the behavior of PTA (more basic than TPPTS) and its benzylated derivative *N*-Bz-PTA (*N*-Bz-PTA = 1-benzyl-1-azonia-3,5-diaza-7-phosphaadamantyl chloride, **14**, less basic than PTA) when mixed with randomly methylated β-CDs (RAME-β-CD) under catalytic conditions [14]. The *N*-benzylated ligand was synthesized in a straightforward way by reaction of PTA with benzyl chloride in methanol under reflux. The product was obtained as a crystalline white compound after workup and recrystallization (Scheme 7).

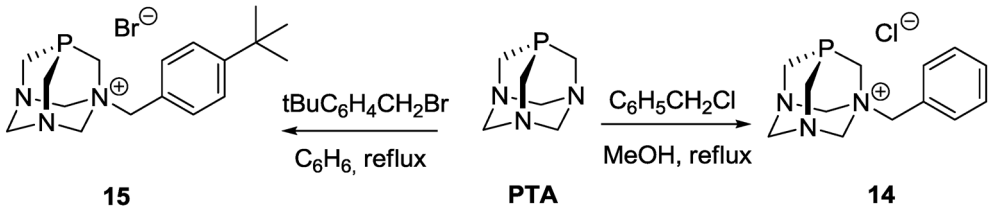

Scheme 7 Synthesis of lower-rim PTA derivatives **14** and **15**.

The lack of interaction between PTA, (*N*-Bz-PTA)Cl, and RAME-β-CD was determined by a spectral displacement method (UV–vis spectroscopy) using methyl orange as a competitor of the ligand. This result was unexpected and in contrast with the large association constant values reported in the literature between CDs and adamantyl derivatives such as adamantyl carboxylic acid for which an association constant K_{ass} = 42 000 M^{-1} was measured [15]. The reason for this behavior is likely due to the hydrophilic character of PTA and (*N*-Bz-PTA)Cl imparted by the three nitrogen of the bottom rim, allowing for extensive hydrogen bonding with water and solvation, thus decreasing the interaction with the lipophilic cavity of CDs.

The degree of ligand inclusion phenomenon could also be assessed by 2D-ROESY (rotating frame Overhauser effect spectroscopy) NMR technique for RAME-β-CD and the less encumbered native β-CD. Whereas no interaction was observed for RAME-β-CD, association constants K_{ass} = 63 and 11 M^{-1} were measured with native β-CD for PTA and (*N*-Bz-PTA)Cl, respectively. On the basis of

these studies, both ligands were tested in the rhodium(I)-catalyzed hydroformylation of long-chain terminal alkenes such as 1-decene in the presence of RAME-β-CD (vide infra).

Another interesting approach to improve the catalytic performances of a rhodium-catalyzed hydroformylation of higher olefins consisted in using amphiphilic phosphines. However, their high surface activity can hamper the decantation process of the biphasic system at the end of the reaction due to emulsion formation. Thus, further tailored modifications of our ligand system were necessary. In principle, the amphiphilic character of a phosphine can be enhanced or decreased depending on the temperature by addition in the medium of a supramolecular receptor in which the phosphine can be included. In this way, a higher phosphine surface activity is expected at high temperature with beneficial effects on the catalytic performances. At the end of the catalytic run, by decreasing the temperature a lower proportion of non-included phosphine should be present in the reaction mixture, with a drop of the surface activity, thus favoring decantation between the aqueous and organic phase (Fig. 1) [16].

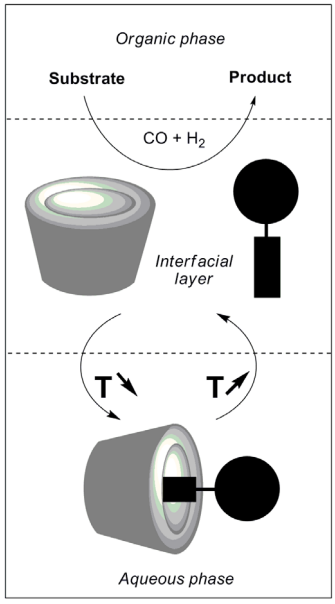

Fig. 1 The principle of thermocontrolled catalysis using a receptor/phosphine couple. P: amphiphilic phosphine. Cat.: organometallic catalyst. Reproduced from ref. [16] by permission of The Royal Society of Chemistry.

The synthetic strategy was therefore to modify (*N*-Bz-PTA)Cl by introducing a substituent that was known to be recognized by the cavity of CDs, such as *tert*-butyl. This was easily achieved by reacting PTA with 4-*tert*-butylbenzyl bromide, giving the novel lower-rim PTA derivative (*N*-^{t}BuBz-PTA)Br (**15**), shown in Scheme 7.

The inclusion of **15** by CDs was determined by 2D T-ROESY NMR experiments (Fig. 2). At room temperature and 80 °C, correlations were detected in the 2D T-ROESY spectra of equimolar mixtures of RAME-β-CD or native β-CD and ligand **15**. Cross-peaks between the *tert*-butyl protons and the H-3, H-5, and H-6 CD protons confirmed deep inclusion of the *tert*-butyl group in the CD cavity.

The association constant was determined by isothermal titration calorimetry (ITC) at 80 °C, the lowest temperature used in catalysis (vide infra). Whereas no association constants could be measured between RAME-β-CD and *N*-Bz-PTA at 80 °C, the RAME-β-CD/**15** and native β-CD/**15** interactions gave the moderately high values K_{ass} = 5440 and 4930 M^{-1}, respectively.

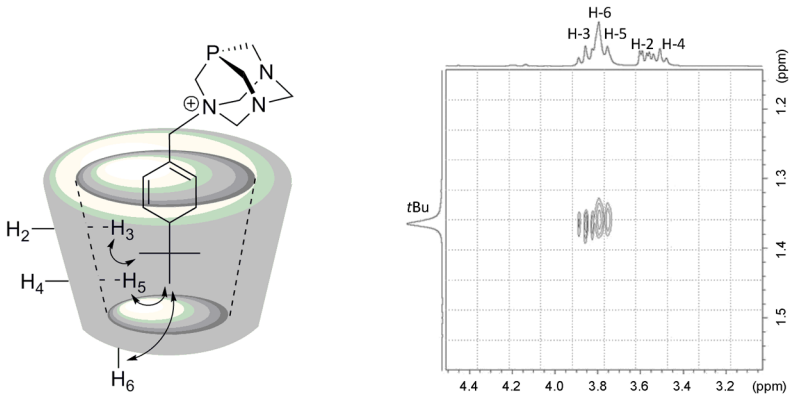

Fig. 2 Labeling scheme and partial 2D T-ROESY NMR spectrum of an equimolar mixture of native β-CD and **15** (D_2O, RT, mixing time = 300 ms, species concentration = 10 mM). Reproduced from ref. [16] by permission of The Royal Society of Chemistry.

Biphasic catalytic hydroformylations with rhodium(I)/CD and lower-rim PTA derivatives

We carried out catalytic experiments to evaluate the performances of PTA, **14** and **15** as water-soluble stabilizing ligands in the rhodium-catalyzed hydroformylation of 1-decene in the presence of RAME-β-CD under biphasic conditions. The results were compared with the benchmark TPPTS as water-soluble phosphine. 1-Decene has been mostly used as model substrate for its hydrophobic character, although higher terminal olefins were also tested [14,16].

The reactions were performed in water at various temperatures using [Rh(acac)$(CO)_2$] as metal precursor, under 50 bar CO/H_2 for 6 h. Selected results are summarized in Table 4.

Table 4 Selected data for biphasic rhodium-catalyzed hydroformylation of 1-decene using PTA and **14**.

Entry	Phosphine	Cyclodextrin	Temperature (°C)	Conversion (%)[b]	Selectivity (%)[c]	l/b ratio[d]
1	TPPTS	RAME-β-CD	80	95	96	1.8
2	TPPTS	RAME-β-CD	100	100	88	1.9
3	TPPTS	RAME-β-CD	120	100	73	2.2
4	PTA	–	80	<1	n.d.	n.d.
5	PTA	–	120	81	96	1.9
6	PTA	RAME-β-CD	80	<1	n.d.	n.d.
7	PTA	RAME-β-CD	100	11	98	1.9
8	PTA	RAME-β-CD	120	94	99	1.7
9	**14**	–	80	19	98	1.9
10	**14**	–	100	77	99	1.8
11	**14**	RAME-β-CD	80	24	98	1.9
12	**14**	RAME-β-CD	100	86	96	1.8

[a]*Experimental conditions*: Rh(acac)$(CO)_2$ (4.07×10^{-2} mmol), water-soluble ligand (0.21 mmol), CD (0.48 mmol), H_2O (11.5 mL), 1-decene (20.35 mmol), 1500 rpm, CO/H_2 (1/1): 50 bar, time: 6 h.

[b]Calculated with respect to the starting olefin.

[c](Mol of aldehydes)/(mol of converted olefins) × 100. The side products were mainly isomeric olefins.

[d]Ratio of linear to branched aldehyde product. Reprinted (adapted) from ref. [14]. Copyright © 2009, with permission from Elsevier.

The main problems with the use of TPPTS, due to its large association constant with CDs, were the increasing amount of alkene isomerization at increasing temperature and a decrease of the linear to branched aldehyde ratio (l/b) already at 80 °C. PTA, being more basic than TPPTS, required higher temperature to generate the active catalytic species (Table 4, entries 4–8). At 120 °C, a conversion of 81 % was measured after 6 h with PTA without RAME-β-CD (Table 4, entry 5). Addition of RAME-β-CD to a PTA-containing catalytic solution resulted in a higher conversion (94 %) at 120 °C (Table 4, entry 8). In contrast to the decrease in chemoselectivity observed with TPPTS at higher temperature, increasing the temperature with PTA as ligand did not alter the chemoselectivity. Indeed, 98 and 99 % aldehydes were formed during the course of the reaction at 100 and 120 °C, respectively, along with small amounts of isomerized alkenes (Table 1, entries 7–8). The l/b ratio remained unchanged with PTA in spite of the presence of RAME-β-CD. When **14** was used instead of PTA, the conversion was higher than that obtained with PTA as expected for a more acidic and surface-active character (Table 4), so the catalytic runs could be carried out at 80 °C with very high chemoselectivity. At 100 °C the conversion of 1-decene was higher as expected, without a loss in chemoselectivity.

An interesting thermoregulation effect was instead observed in the presence of **15**. At 80 °C without CD, **15** gave a conversion close to that obtained with **14** in the hydroformylation of 1-decene (26 vs. 19 %, respectively), however, higher than with TPPTS (3 % conversion). Unexpectedly, at 80 °C however, addition of excess RAME-β-CD to a reaction mixture containing **15** led to a drop in the catalytic activity (from 26 to 10 % conv.). This was also the case when 1-dodecene (from 39 to 11 % conv.) and 1-tetradecene (from 53 to 14 % conv.) were used as substrates (Table 5). By raising the temperature to 100 and 120 °C, addition of excess RAME-β-CD resulted instead in an increase in catalytic activity, namely, from 56 to 72 % for 1-decene at 100 °C, from 49 to 75 % for 1-dodecene and from 53 to 88 % for 1-tetradecene, respectively. It was concluded that the presence of RAME-β-CD could affect the conversion either positively or negatively depending on the reaction temperature, indicative of a temperature-dependent variation of the association constant between RAME-β-CD and **15**. Thus, at higher temperatures, an increase of "free" RAME-β-CD concentration in solution had to be expected. An indirect

Table 5 Selected data for biphasic rhodium-catalyzed hydroformylation of higher olefins using **15**.

Entry	Olefin	Phosphine	Cyclodextrin	Temperature (°C)	Conversion (%)[b]	Selectivity (%)[c]	l/b ratio[d]
5	1-Decene	**15**	–	80	26	99	2.1
6	1-Decene	**15**	RAME-β-CD	80	10	97	1.8
7	1-Decene	**15**	Native β-CD	80	9	97	1.9
8	1-Decene	**15**	–	100	56	99	1.7
9	1-Decene	**15**	RAME-β-CD	100	72	99	2.0
10	1-Decene	**15**	Native β-CD	100	67	95	1.8
11	1-Decene	**15**	–	120	94	99	1.9
12	1-Decene	**15**	RAME-β-CD	120	98	99	1.8
13	1-Dodecene	**15**	–	100	49	98	1.5
14	1-Dodecene	**15**	RAME-β-CD	100	75	99	1.7
15	1-Dodecene	**15**	Native β-CD	100	71	98	1.6
16	1-Tetradecene	**15**	–	100	57	97	1.5
17	1-Tetradecene	**15**	RAME-β-CD	100	88	97	1.9
18	1-Tetradecene	**15**	Native β-CD	100	66	98	1.7

[a]Experimental conditions: $Rh(acac)(CO)_2$ (4.07×10^{-2} mmol), water-soluble ligand (0.21 mmol), CD (0.48 mmol), H_2O (11.5 mL), 1-alkene (20.35 mmol), 1500 rpm, CO/H_2 (1/1): 50 bar, 6 h.

[b]Calculated with respect to the starting olefin.

[c](Mol of aldehydes)/(mol of converted olefins) × 100. The side products were mainly isomeric olefins.

[d]Ratio of linear to branched aldehyde product. Reproduced (adapted) from ref. [16] by permission of The Royal Society of Chemistry.

proof of this behavior was obtained by replacing RAME-β-CD by the less encumbered native β-CD. At 80 °C, the native β-CD/**15** association constant (K_{ass} = 4930 M^{-1}) was similar to that measured for RAME-β-CD. This in turn agrees with the only slight difference observed in the conversion of 1-tetradecene between the native β-CD and RAME-β-CD at 80 °C (11 vs. 14 %). Running the tests at 100 °C instead, a significant variation in conversion was obtained (66 vs. 88 % conv.).

A practical use of this thermoregulatory effect was to solve the problem of emulsions. In the presence of **15**, the decantation was on the order of several seconds, whereas hours are needed with **14**. This can be due to the fact that by decreasing the temperature at the end of the reaction, inclusion of **15** in the RAME-β-CD cavity and coordination of **15** to rhodium can occur (Fig. 3), giving a loss in surface activity and rapid decantation. Thus, the products and the rhodium catalyst could be easily recovered in two distinct phases.

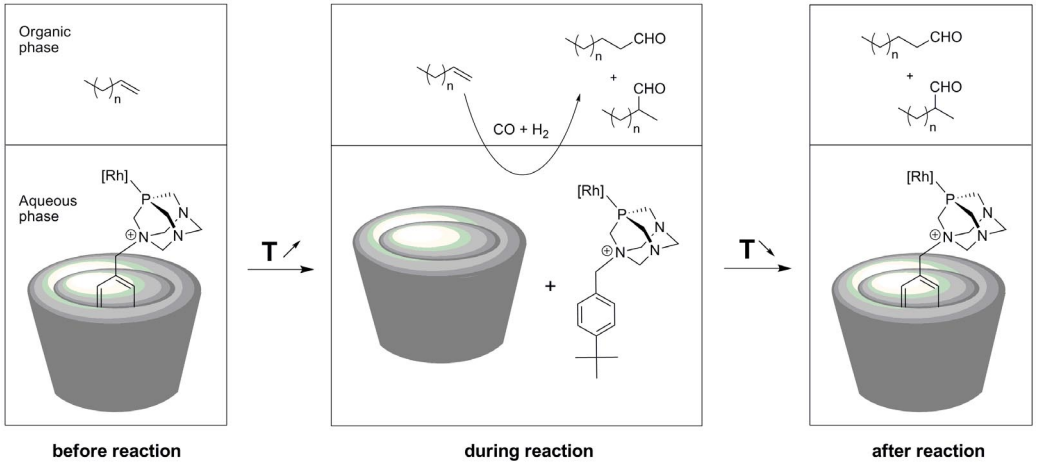

Fig. 3 CD-**15** interaction and effect in a thermocontrolled hydroformylation of higher olefins. Reproduced from ref. [16] by permission of The Royal Society of Chemistry.

CONCLUSIONS

In this review article we have shown that PTA can be used as a versatile scaffold for tailored synthetic modifications, giving small libraries of "upper" and "lower" rim derivatives, endowed with interesting properties that were exploited in C=C and C=O bond hydrogenations and higher olefins hydroformylations. Our collaborative work is being continued to design other solutions for specific problems linked to catalyzed reactions in water or biphasic systems.

ACKNOWLEDGMENTS

This research was supported by the Centre National de la Recherche Scientifique (CNRS) and Consiglio Nazionale delle Ricerche (CNR), also through the bilateral CNR-CNRS agreement 2010–2011. Ente Cassa di Risparmio di Firenze (ECRF), MIUR, MATTM are thanked for financial support through projects HYDROLAB, EFOR, PRIN 2009, and PIRODE. COST Action CM0802 "PhoSciNet" is also thanked for additional support. LG thanks MAE for a JRP grant within the Executive Programme of Cooperation Italy-USA (2008–2009). DAK thanks the American Chemical Society Petroleum Research Fund (Grant 49372-UFS) and Fulbright Research Scholarships (2009–2010) for partial support of this research.

REFERENCES

1. (a) D. J. Daigle, A. B. Pepperman Jr., S. L. Vail. *J. Heterocycl. Chem*. **11**, 407 (1974); (b) D. J. Daigle. *Inorg. Synth*. **32**, 40 (1998).
2. (a) A. D. Phillips, L. Gonsalvi, A. Romerosa, F. Vizza, M. Peruzzini. *Coord. Chem. Rev.* **248**, 955 (2004); (b) J. Bravo, S. Bolaño, L. Gonsalvi, M. Peruzzini. *Coord. Chem. Rev*. **254**, 555 (2010).
3. (a) S. Bolaño, L. Gonsalvi, F. Zanobini, F. Vizza, V. Bertolasi, A. Romerosa, M. Peruzzini. *J. Mol. Catal. Chem. A* **224**, 61 (2004); (b) H. Horváth, G. Laurenzy, A. Katho. *J. Organomet. Chem*. **689**, 1036 (2004); (c) C. A. Mebi, B. J. Frost. *Organometallics* **24**, 2339 (2005); (d) D. A. Krogstad, J. Cho, A. J. DeBoer, J. A. Klitzke, W. R. Sanow, H. A. Williams, J. A. Halfen. *Inorg. Chim. Acta* **359**, 136 (2006); (e) D. A. Krogstad, S. B. Owens, J. A. Halfen, V. G. Young Jr. *Inorg. Chem. Commun*. **8**, 65 (2005); (f) D. A. Krogstad, A. J. DeBoer, W. J. Ortmeier, J. W. Rudolf, J. A. Halfen. *Inorg. Chem. Commun.* **8**, 1141 (2005); (g) C. A. Mebi, R. P. Nair, B. J. Frost. *Organometallics* **26**, 429 (2007).
4. (a) W. H. Ang, E. Daldini, C. Scolaro, R. Scopelliti, L. Juillerat-Jennerat, P. J. Dyson. *Inorg. Chem.* **45**, 9006 (2006); (b) C. Scolaro, A. Bergamo, L. Brescacin, R. Delfino, M. Cocchietto, G. Laurenczy, T. J. Geldbach, G. Sava, P. J. Dyson. *J. Med. Chem*. **48**, 4161 (2005); (c) A. Dorcier, W. H. Ang, S. Bolaño, L. Gonsalvi, L. Juillerat-Jennerat, G. Laurenczy, M. Peruzzini, A. D. Phillips, F. Zanobini, P. J. Dyson. *Organometallics* **25**, 4090 (2006); (d) A. Casini, F. Edafe, M. Erlandsson, L. Gonsalvi, A. Marrone, A. Ciancetta, N. Re, A. Ienco, L. Messori, M. Peruzzini, P. J. Dyson. *Dalton Trans*. **39**, 5556 (2010).
5. V. Gutkin, J. Gun, P. V. Prikhodchenko, O. Lev, A. Romerosa, T. Campos Malpartida, C. Lidrissi, L. Gonsalvi, M. Peruzzini. *J. Electrochem. Soc.* **154**, F7 (2007).
6. (a) A. Rossin, L. Gonsalvi, A. D. Phillips, O. Maresca, A. Lledos, M. Peruzzini. *Organometallics* **26**, 3289 (2007); (b) G. Kovacs, A. Rossin, L. Gonsalvi, A. Lledos, M. Peruzzini. *Organometallics* **29**, 5121 (2010).
7. G. W. Wong, J. L. Harkreader, C. A. Mebi, B. J. Frost. *Inorg. Chem*. **45**, 6748 (2006).
8. (a) M. Erlandsson, L. Gonsalvi, A. Ienco, M. Peruzzini. *Inorg. Chem*. **47**, 8 (2008); (b) G. W. Wong, W.-C. Lee, B. J. Frost. *Inorg. Chem*. **47**, 612 (2008).
9. A. Guerriero, M. Erlandsson, D. A. Krogstad, A. Ienco, M. Peruzzini, G. Reginato, L. Gonsalvi. *Organometallics* **30**, 1874 (2011).
10. D. A. Krogstad, A. Guerriero, A. Ienco, G. Manca, M. Peruzzini, G. Reginato, L. Gonsalvi. *Organometallics* **30**, 6292 (2011).
11. (a) C. W. Kohlpaintner, R. W. Fischer, B. Cornils. *Appl. Catal. A: Gen.* **221**, 219 (2001); (b) B. Cornils, E. G. Kuntz. *J. Organomet. Chem*. **502**, 177 (1995).
12. F. Hapiot, L. Leclercq, N. Azaroual, S. Fourmentin, S. Tilloy, E. Monflier. *Curr. Org. Synth*. **5**, 162 (2008).
13. E. Monflier, H. Bricout, F. Hapiot, S. Tilloy, A. Aghmiz, A. M. Masdeu-Bultó. *Adv. Synth. Catal*. **346**, 425 (2004).
14. F.-X. Legrand, F. Hapiot, S. Tilloy, A. Guerriero, M. Peruzzini, L. Gonsalvi, E. Monflier. *Appl. Catal. A: Gen.* **362**, 62 (2009).
15. C. Binkowski, F. Hapiot, V. Lequart, P. Martin, E. Monflier. *Org. Biomol. Chem.* **3**, 1129 (2005).
16. N. Six, A. Guerriero, D. Landy, M. Peruzzini, L. Gonsalvi, F. Hapiot, E. Monflier. *Catal. Sci. Technol*. **1**, 1347 (2011).

